JACS
JOURNAL OF THE AMERICAN CHEMICAL SOCIETY

ARTICLE

pubs.acs.org/JACS

Alkali Metals in Ethylenediamine: A Computational Study of the Optical Absorption Spectra and NMR Parameters of $[M(en)_3^{\delta+}\cdot M^{\delta-}]$ Ion Pairs

Eva Zurek

Department of Chemistry, State University of New York at Buffalo, 331 Natural Sciences Complex, Buffalo, New York 14260, United States

Supporting Information

ABSTRACT: The optical absorption spectra of alkali metals in ethylenediamine have provided evidence for a third oxidation state, −1, of all of the alkali metals heavier than lithium. Experimentally determined NMR parameters have supported this interpretation, further indicating that whereas Na^- is a genuine metal anion, the interaction of the alkali anion with the medium becomes progressively stronger for the larger metals. Herein, first-principles computations based upon density functional theory are carried out on various species which may be present in solutions composed of alkali metals and ethylenediamine. The energies of a number of hypothetical reactions computed with a continuum solvation model indicate that neither free metal anions, M^-, nor solvated electrons are the most stable species. Instead, $[Li(en)_3]_2$ and $[M(en)_3^{\delta+}\cdot M^{\delta-}]$ (M = Na, K, Rb, Cs) are predicted to have enhanced stability. The $M(en)_3$ complexes can be viewed as superalkalis or expanded alkalis, ones in which the valence electron density is pulled out to a greater extent than in the alkali metals alone. The computed optical absorption spectra and NMR parameters of the $[Li(en)_3]_2$ superalkali dimer and the $[M(en)_3^{\delta+}\cdot M^{\delta-}]$ superalkali−alkali mixed dimers are in good agreement with the aforementioned experimental results, providing further evidence that these may be the dominant species in solution. The latter can also be thought of as an ion pair formed from an alkali metal anion (M^-) and solvated cation ($M(en)_3^+$).

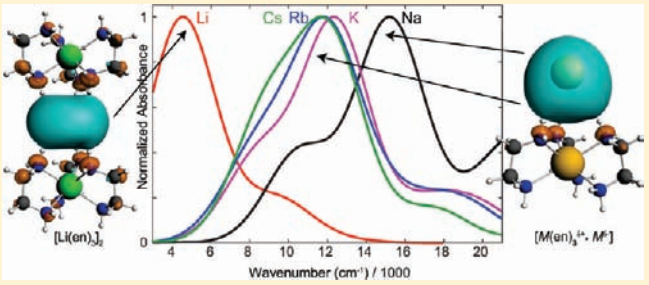

1. INTRODUCTION

On November of 1808 Sir Humphry Davy poetically described the first observation of alkali metals dissolved in gaseous ammonia in his laboratory notebook.[1−3] These findings were not published however, and the phenomenon remained quiescent until one-half a century later when Weyl independently documented very similar observations.[4] Ever since Weyl's discovery, great fascination has ensued with the properties of these and conceptually related systems: solvated electrons, electrides, expanded metals, alkalides,[5−13] and excess electrons in water.[14−17]

One of the most intriguing aspects of metal−ammonia solutions (MAS) is the metal-independent optical absorption spectrum of the dilute, blue solutions.[18−22] All of the alkalis as well as calcium and strontium, europium, and yterbium give rise to nearly indistinguishable absorption curves. Similar bands are found in the radiolysis of *only* liquid ammonia.[23] The spectra are characterized by a single absorption band, centered around 0.8−0.88 eV, and a long tail (the source of the blue color) which trails off to about 1.8 eV.[24] This is the spectral signature of the solvated electron. In 1959 Jortner put forward a model which has profoundly shaped our understanding of this exotic species.[25] He thought of the solvated electron as being trapped in a spherical cavity made up of ammonia molecules. Assuming that the surrounding solvent was a continuous homogeneous medium and a cavity radius of 3−3.2 Å, Jortner calculated the energy of the ground 1s and first excited 2p states of an electron in this cavity. The absorption between the two gave a 1s → 2p transition of 0.8 eV, in excellent agreement with the absorption maxima characteristic of all MAS. Extensions to this model have attempted to describe the line shape as well as the concentration and temperature dependence of the spectrum.[26]

Recently, we performed an extensive computational study of the numerous species which may be present in lithium−ammonia solutions.[5] The TD-DFT optical absorption spectra of various ion pairs (models for the solvated electron) showed that the three most intense electronic excitations arise from the transition from the SOMO (of s pseudosymmetry) into the lowest lying p-like levels, in accordance with the Jortner model. The long tail which extends into the visible was attributed to transitions to levels higher in energy. The spectra were found to be relatively metal independent, with a hint of a red shift moving down group I. Interestingly, our computations indicated that

Received: September 21, 2010
Published: March 02, 2011

$Li(NH_3)_4$ may also be a chromophore in MAS. This prediction has been confirmed experimentally by Varriale et al., who also showed that the electronic spectrum of $Li(NH_3)_4$ exhibits rich vibrational structure.[27]

Despite the low solubility, dilute solutions of alkali metals in other amines and ethers can also be made.[8,9,13] The spectra obtained in these solvents differs drastically from those of MAS, providing evidence for the existence of yet another unusual species: *alkali metal anions* (M^-).[28−31] The spectra of potassium, rubidium, and cesium in ethylenediamine[30,32] consist of a shoulder ascribed to solvated electrons and a metal-dependent band attributed to K^-, Rb^-, and Cs^-. The sodium solutions show only a band arising from Na^-, whereas those with lithium provide evidence solely for solvated electrons. Pulse radiolysis of pure ethylenediamine yields spectra which are nearly identical to those attributed to the solvated electron in alkali metal solutions.[23] About 160 years after Davy's discovery of sodium and potassium it was proposed that in addition to the usual 0 and +1 oxidation states, the alkali metals may have a third oxidation state of −1.[13]

The solubility of these solutions can be greatly enhanced by adding crown ethers or cryptands.[8−11,13] In fact, the nuclear magnetic resonance (NMR) of $^{23}Na^-$ in solutions containing the 2,2,2-cryptand were the first to provide evidence that the sodide is a genuine anion.[33] Since then, NMR has been used to identify $^{23}Na^-$, $^{39}K^-$, $^{87}Rb^-$, and $^{133}Cs^-$ in a variety of different solvents.[34−37] The NMR spectra of crystalline salts such as $Li^+(en)_2 \cdot Na^-$ have also been measured.[38] A comparison of the calculated chemical shift difference between the gaseous metal anion and the neutral atoms, with those observed experimentally for the anions in solution, has shed light on the strength of the interaction between the anion and the solvent.[39] Whereas Na^- was found to interact weakly with its environment, Rb^- and Cs^- were significantly perturbed by the solvent and K^- was intermediate in character.

Herein, we build upon the insights gained in our previous studies on MAS[5] and attempt to understand the peculiarities of alkalis in ethylenediamine (en). The DFT energies of a number of reactions have been computed using a continuum solvation model. Systems which can be thought of as dimers of superatoms, $[Li(en)_3]_2$, or superalkali−alkali complexes with the formula $[M(en)_3^{\delta+} \cdot M^{\delta-}]$ (M = Na, K, Rb, Cs) are found to be particularly stable. The computed absorption spectra and NMR chemical shifts of the species we propose to be dominant in solution agrees well with those obtained experimentally.

2. COMPUTATIONAL DETAILS

The computational settings have been chosen to resemble those from ref 5 as closely as possible, since they were found to perform well for the geometries, relative energies, and optical absorption spectra of the various species likely to be present in MAS. We used the Amsterdam Density Functional (ADF) package,[40,41] the revPBE nonhybrid gradient density functional,[42−45] along with the VWN[46] local spin density approximation (LSDA). The basis functions on nitrogen and carbon consisted of a valence triple-ζ Slater-type basis set with polarization functions (TZP) and a 1s frozen core from the ADF basis-set library. Our previous studies showed that in order to properly describe the various species present in MAS it was necessary to use diffuse basis sets on H, for which an all-electron even-tempered valence quadruple-ζ basis set with 3 polarization functions and 1 set of diffuse s, p, d, and f STOs (ET-QZ3P(1)) was employed. For the alkalis the quadruple-ζ Slater-type basis set with polarization functions (QZ4P) and the ET-QZ3P(1) basis sets give very similar results (the relative energies of various species differed by only a few tenths of a kcal/mol). The values provided in the main text were obtained using an ET-QZ3P(1) basis for the lighter alkalis and a ZORA relativistic QZ4P basis along with the zeroth-order regular approximation (ZORA) Hamiltonian[47−49] for Rb and Cs. For a number of representative systems the Counterpoise method was employed to determine the basis-set superposition error (BSSE), which was found to be small, on the order of a few tenths of a kcal/mol. Approximate DFT functionals suffer from self-interaction error, which causes an artificial delocalization of the electron density.[50] Our previous results on $Li(NH_3)_4$[5] agreed with those obtained from MP2 calculations,[51] suggesting that for these classes of systems and the aforementioned computational settings the delocalization error is likely to be small.

Vertical excitation energies were calculated using TD-DFT as implemented in ADF[52,53] and the aforementioned basis sets. We also calculated the excitations with the CAM-B3LYP range-separated density functional[54] as implemented in NWChem.[55,56] The 6-311++G** basis set has been employed for H, C, N, Li, Na, and K. For Rb and Cs it was found that the excitations obtained using a standard TZVP basis[57] (and the corresponding ECP) were nearly identical to those obtained with a TZVP basis to which an extra SP set of diffuse functions was added. The choice of functional did not have a substantial effect on the maxima in the simulated absorption spectra. However, a number of spurious, low-energy excitations resulting from the well-known tendency of TD-DFT to overstabilize charge-transfer states were computed with revPBE. Thus, the simulated spectra shown in the main text were obtained from the excitations computed with the CAM-B3LYP functional.

The effects of solvation were approximated macroscopically by the COSMO method[58−60] as implemented in ADF.[61] Full geometry optimizations were carried out using the solvent excluding surface, a dielectric constant of 13.5, and hard-sphere radius of 3.5 Å for ethylenediamine (en). Atomic radii of 1.16/1.4/2.0/1.5/1.9/2.3/2.5/2.7 Å were used for H/N/C/Li/Na/K/Rb/Cs. The Δ*E*s given in the text (gas and solution phase, ΔE_{gas}, ΔE_{solv}, respectively) are energy differences (products minus reactants) for specified reactions. They do not include zero-point or vibrational finite temperature corrections. The ΔE_{solv} values were calculated with energies obtained from optimizations carried out with COSMO. We estimate that the various parameters used in the COSMO calculations will have a greater influence on ΔE_{solv} than does the BSSE.

The orbital isoprobability diagrams and contour plots have been calculated in the gas phase. The former were obtained using the procedure described in ref 62, which has also been employed in studies of anionic water clusters.[15] The orbital numbering excludes the N and C 1s frozen cores. The initial geometries of a few of the molecules have been constructed with C_3 symmetry. Since this point group is not supported by ADF, calculations were carried out using C_1 symmetry instead.

The NMR chemical shieldings of the lighter alkalis (Li, Na, K) were obtained with the nonrelativistic GIAO (gauge-including atomic orbitals) methodology developed by Schreckenbach and Ziegler[63,64] as implemented in the "NMR" program of the ADF package. For Rb and Cs, relativistic computations of the nuclear shielding constants based on the zeroth-order regular approximation (ZORA) Hamiltonian were carried out.[47,65] For the heavier alkalis spin−orbit coupling was not considered, as it has been demonstrated that these contributions will cancel out in chemical shift calculations.[66]

3. RESULTS AND DISCUSSION

3.1. Alkali Metal−Ethylenediamine Complexes. The lithium cation and atom can coordinate up to four ammonia molecules in a tetrahedral fashion.[5] In order to determine the preferred mode of coordination between ethylenediamine and

dx.doi.org/10.1021/ja1085244 |*J. Am. Chem. Soc.* 2011, 133, 4829–4839

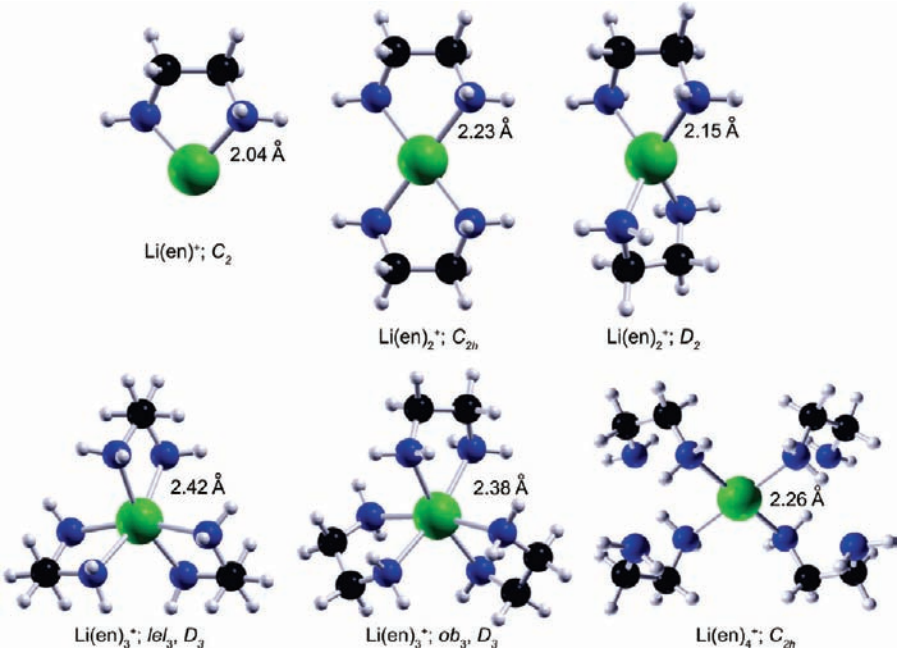

Figure 1. Optimized geometries of $Li(en)_n^+$ (n = 1−4) complexes. The gas-phase Li−N distances are also provided.

Table 1. Gas-Phase Change in Energy, ΔE_{gas} in kcal/mol, for the Reaction $M^+ + n(en) \rightarrow M(en)_n^+$ [a]

n	$Li(en)_n^+$	$Na(en)_n^+$	$K(en)_n^+$	$Rb(en)_n^+$	$Cs(en)_n^+$
1	−66.6 (−20.2)	−45.4 (−15.1)	−31.0 (−8.5)	−26.0 (−6.3)	−22.3 (−5.3)
2	−105.6 (−34.8)	−75.4 (−25.1)	−52.1 (−12.6)	−43.6 (−8.9)	−36.9 (−5.9)
3	−110.5 (−29.9)	−88.7 (−28.8)	−65.1 (−16.6)	−55.1 (−8.9)	−46.8 (−4.6)
4	−106.6 (−11.9)	−83.9 (−9.5)	−66.2 (−5.4)	−57.1 (−1.5)	−49.9 (1.9)

[a] Here, en = ethylenediamine; M = Li, Na, K, Rb, Cs, and n = 1−4. The solution-phase values, ΔE_{solv}, are given in parentheses. For n = 2 two isomers have been considered as shown in Figure 1. For n = 3 the ob_3 and the lel_3 conformers were examined. The values provided are for the most stable structure.

the alkali metals, the geometries of various $M(en)_n^+$ (M = Li−Cs; n = 1−4) complexes have been optimized. Initial computations on $Na(en)^+$ and Na(en) confirmed the expectation that ethylenediamine prefers to coordinate to the metal in a bidendate fashion. Accordingly, structures similar to those illustrated in Figure 1 (which shows the optimized geometries for the systems where M = Li) were considered.

For n = 2, computations were carried out on two isomers. In the case of the smaller alkalis (Li, Na, K), the complex with D_2 symmetry was found to be lower in energy, for Rb the two were isoenergetic, and for Cs the C_{2h} system was preferred. The energy differences between the two isomers were typically less than 1 kcal/mol, suggesting that their interconversion will be facile.

It was assumed that $M(en)_3^+$ would adopt a structure similar to the chiral coordination complex $[Co(en)_3]^{3+}$ with D_3 symmetry. Both the Δ and the Λ stereoisomer can have four conformers, which may be distinguished by the orientation of the plane of the chelate rings: either parallel (*lel*) or oblique (*ob*) with respect to the C_3 axis of the molecule. For $[Co(en)_3]^{3+}$, the energy differences are rather small: the ob_3 conformer has been computed to be more stable than lel_3 by ∼1 kcal/mol,[67,68] with the energy of the ob_2lel and the lel_2ob falling between these two.[68] For the systems considered herein, the difference between ob_3 and lel_3 is also found to be minimal, less than 0.3 and 3.5 kcal/mol in the gas and solution phase. It is therefore expected that at room temperature all four conformers will be present, and the chelate rings will rapidly interconvert between the different orientations.

In the optimization of $M(en)_4^+$ the starting geometry was chosen such that all four ethylenediamine molecules were coordinated to the metal in a bidendate fashion. For Li and Na four of the M−N bonds broke (d > 3.8 Å) during the optimization, hinting that the smaller alkalis can coordinate up to six nitrogen atoms. It is likely that other conformers of $M(en)_4^+$ may have similar energies as well.

The formation energies of these complexes are given in Table 1. Adding the second ligand to the metal was found to be less exothermic than coordination with the first. Reaction with the third ethylenediamine molecule was still exothermic (in the gas phase), whereas formation of $M(en)_4^+$ was only slightly favorable for the larger metals K, Rb, and Cs. The strength of the interaction with the ligand was found to decrease as the size of the metal increased.

The solution-phase data predict that formation of $M(en)_3^+$ from $M(en)_2^+$ will be (slightly) exothermic only for K and Na. Except for Li, the destabilization is small. The values obtained from the COSMO calculations should be taken with a grain of salt since they depend on various parameters, such as the radii of the atoms and of the solvent molecule, as well as the type of surface used to create the cavity. As expected, the trends show that small, charged species are stabilized in solution.

These results suggest that the metal cations will coordinate with around three ethylenediamine molecules. An approximate MO (molecular orbital) interaction diagram for the formation of $Li(en)_3^+$ is illustrated in Figure 2 (the heavier metals gave results which were qualitatively similar). The diagram was obtained from a restricted calculation on the neutral complex, but the occupation shown is for the cation. The block of orbitals $13e_1$, $6a_2$, $12e_1$, and $8a_1$ arise from the interactions of the HOMO (highest occupied MO), HOMO−1, and HOMO 2 of the three

dx.doi.org/10.1021/ja1085244 |J. Am. Chem. Soc. 2011, 133, 4829–4839

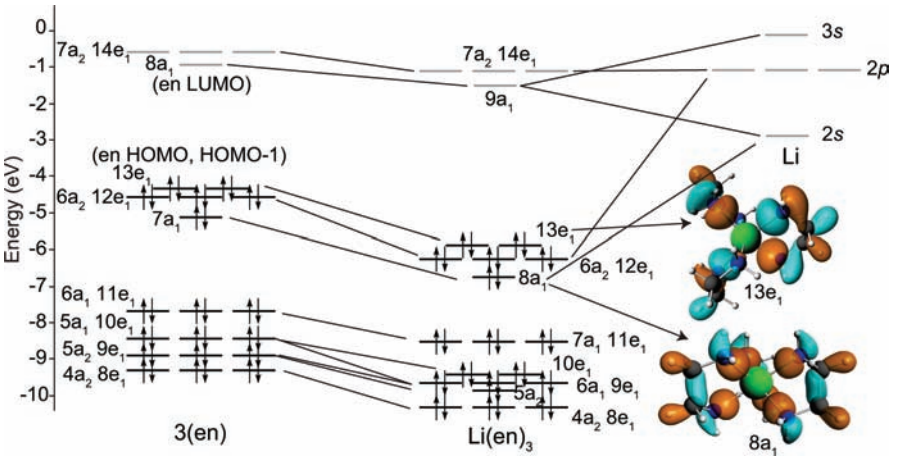

Figure 2. Approximate interaction diagram for the formation of $Li(en)_3$ from Li and three ethylenediamine molecules. The electron occupation shown is for the cation. Isosurfaces of the $8a_1$ and one of the two degenerate $13e_1$ orbitals are also provided.

Table 2. Gas-Phase Change in Energy, ΔE_{gas}, in kcal/mol, for the Reaction $M+n(en) \rightarrow M(en)_n$ [a]

n	$Li(en)_n$	$Na(en)_n$	$K(en)_n$	$Rb(en)_n$	$Cs(en)_n$
1	−21.5 (−11.0)	−8.8 (−3.2)	−7.7 (−1.7)	−5.3 (0.4)	−5.3 (0.7)
2	−42.1 (−22.7)	−18.4 (−2.9)	−15.0 (0.5)	−10.3 (4.1)	−9.8 (4.1)
3	−43.4 (−21.7)	−26.6 (−5.0)	−22.8 (−1.9)	−15.9 (6.9)	−13.8 (5.8)
4	−34.3 (1.2)	−19.4 (12.8)	−22.6 (9.6)	−15.8 (15.4)	−14.5 (16.4)

[a] Here, en = ethylenediamine, M = Li, Na, K, Rb, Cs, and $n = 1-4$. The solution-phase values, ΔE_{solv}, are given in parentheses. For $n = 2$ two structures have been considered as shown in Figure 1. For $n = 3$ the ob_3 and the lel_3 conformers were examined. The values provided are for the most stable isomer.

ethylenediamine molecules and have a little bit of symmetry-allowed Li s ($8a_1$), p ($6a_2$, $12e_1$), and d ($13e_1$) character mixed in. Isosurfaces of the completely in-phase $8a_1$ combination and one of the doubly degenerate $13e_1$ HOMOs illustrate that the lone pairs on the nitrogen atoms, and the C−H σ bonds contribute to these MOs. This is in line with what was found previously for the cationic monomer in MAS: the ammonia lone pair contributed substantially to the HOMO of $Li(NH_3)_4^+$.[5]

Neutral $M(en)_n$ (M = Li−Cs; $n = 1-4$) complexes have also been considered, and geometries similar to those illustrated for $Li(en)_n^+$ in Figure 1 were optimized. With the exception of Cs, the most stable $M(en)_2$ and $M(en)_2^+$ isomers had the same symmetry. In accordance with the results for the cation, the energies of the lel_3 and ob_3 conformers of $M(en)_3$ were found to differ by less than 0.5 and 3.0 kcal/mol in the gas and solution phase, respectively. In agreement with the findings obtained for $M(en)_4^+$, four of the Li−N and Na−N bonds broke ($d > 3.4$ Å) during the optimization of $M(en)_4$, indicating that these alkalis can accommodate up to six metal−nitrogen bonds.

Table 2 suggests that Li and Na will coordinate up to three ethylendiamine molecules in the gas phase. Since for the heavier metals $E(M(en)_3)-E(M(en)_4)$, it is also unlikely that a fourth ligand will bind to K, Rb, or Cs. Solvation stabilizes the uncomplexed metal atoms, so that reaction of the heavier metals with the ligands is actually calculated to be endothermic. In complete analogy to what was found for the cations, the interaction of the metals with the ligands becomes weaker as the size of the metal increases. The degree of coordination will

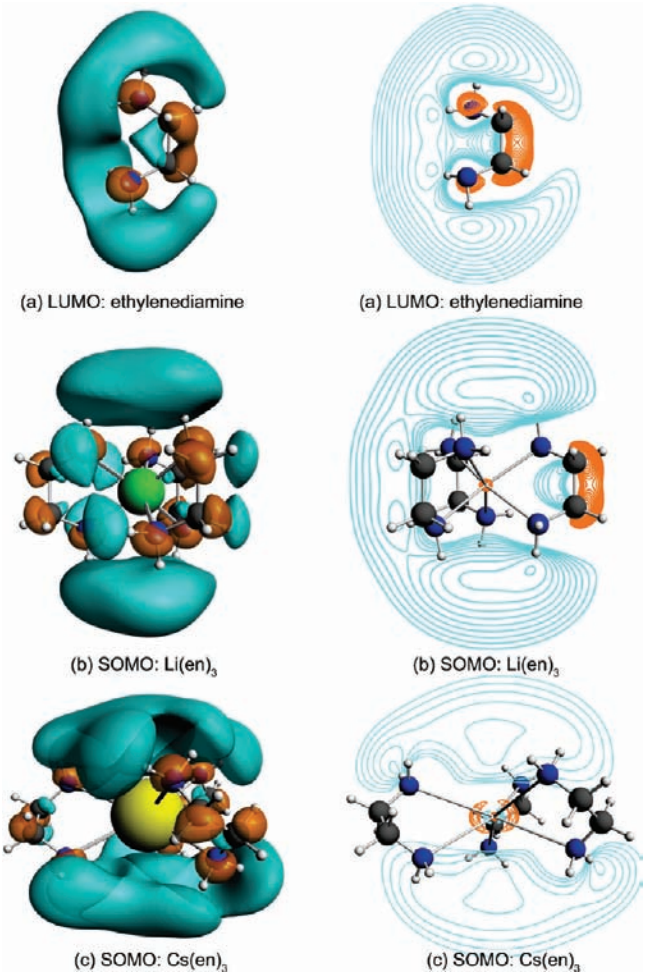

Figure 3. Isoprobability surfaces encompassing 30% of $|\Psi|^2$ of the (a) LUMO of ethylenediamine, (b) SOMO of $Li(en)_3$, and (c) SOMO of $Cs(en)_3$. Also shown are the corresponding contour diagrams where the plane of the contours (a) bisects the two C atoms, (b) contains two C as well as one Li atom, and (c) contains two H and one Cs atom. The metal atoms have been omitted for clarity in the contour diagrams.

depend upon the alkali, the medium, and further reactions (to be studied below) that the $M(en)_n$ entities may undergo. Our focus

dx.doi.org/10.1021/ja1085244 |J. Am. Chem. Soc. 2011, 133, 4829–4839

will be on alkalis chelated by three ethylenediamine molecules since in general these were the most stable neutral and cationic systems in the gas-phase calculations. The following discussion is based upon the results obtained for the lel_3 species. In a room-temperature solution all four conformers will be present. Our computations indicate that the reaction energies, optical absorption spectra, and NMR chemical shieldings of the ob_3 and lel_3 species are very similar, suggesting that those of the ob_2lel and lel_2ob will be comparable as well.

The interaction diagram in Figure 2 is typical for all of the $M(en)_3$ complexes. It shows that the $Li(en)_3$ SOMO (singly occupied MO) of a_1 symmetry is composed of the Li occupied (2s) and unoccupied (3s) functions. Another important contribution arises from an in-phase combination of the ethylenediamine LUMOs (lowest unoccupied MOs) which are very diffuse, Rydberg-like with a node near the hydrogens, see Figure 3a. Partial filling of these LUMOs and their overlap results in orbital-mediated bonding between neighboring hydrogen atoms. In our previous work on MAS[5] we gave this a new symbol, H⟵〰⟶H, in order to distinguish it from normal hydrogen bonding. Intermolecular H⟵〰⟶H bonding interactions were also found in the quasispherical $4a_1$ SOMO of the tetrahedral $Li(NH_3)_4$ monomer, and it was noted that this system can be thought of as a superatom. Similar bonding has previously been predicted for negatively charged fluorocarbon cages.[69]

Isoprobability surfaces and contour diagrams of the $Li(en)_3$ and $Cs(en)_3$ SOMOs are provided in Figure 3b and 3c. The former contain 30% of the electron density of the SOMOs.

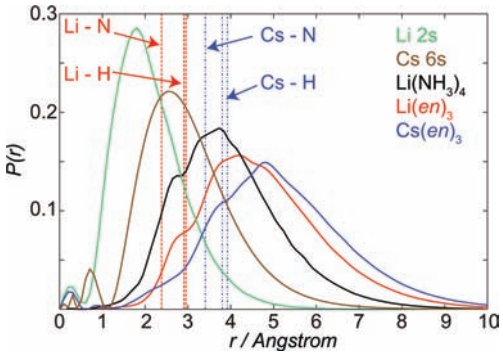

Figure 4. Spherically averaged gas-phase probability, $P(r)$, that the valence electron is a distance r from the metal center in the lithium and cesium atoms as well as in $Li(NH_3)_4$, $Li(en)_3$, and $Cs(en)_3$. For the ethylenediamine complexes the distance between the metal atom and the nitrogens as well as the hydrogens in the NH_2 groups is provided; at around this point, $P(r)$ rises sharply due to the partial filling of the ethylenediamine LUMOs and the resulting H⟵〰⟶H bonding interactions.

Despite the fact that these systems are less spherical than the $Li(NH_3)_4$ molecule, they are still basically s-like, and can be thought of as superatoms or superalkalis. They can also be thought of as expanded metal atoms, ones in which the electron density is pulled further away from the nuclei than in the metal atoms alone. The spherically averaged probability, $P(r)$, to find the electron a distance r from the metal center in Figure 4 illustrates that the degree of "expansion" in $Li(en)_3$ is greater than in $Li(NH_3)_4$ and that the "radius" of the $Cs(en)_3$ superatom is slightly larger than that of $Li(en)_3$. Similar results have been previously obtained for Li(9-crown-3)$_2$.[70] The effect of the degree of expansion on the properties and electronic structure of Li-containing solids has been studied by varying the ligands from ammonia, to methylamine, to [2,1,1] cryptate.[71]

3.2. What Is the Most Stable Species: A Comparison of Possible Reactions. In order to determine the major constituents of alkali−ethylenediamine solutions, a number of possible products of the reaction of two metal atoms with six ethylendiamine molecules (2M + 6(en)) have been considered. The first row in Table 3 shows that formation of a complexed metal cation along with an electron delocalized over a cluster of three ethylenediamine molecules, $e^-@(en)_3$ (the solvated electron), is highly endothermic in the gas phase. Solvation stabilizes the products, yet even then the reaction is energetically favorable only for the lightest alkali metal. In accord with our previous results on electrons solvated in ammonia,[5] the second row reveals that in general for $n = 3$ the $[M(en)_3^+ \cdot e^-@(en)_n]$ ion pairs are more stable than infinitely separated $M(en)_3^+$ and $e^-@(en)_n$ (in the Supporting Information it is shown that for $n = 1$, 6 the formation energies are similar in magnitude). Comparison of the reaction energies in the first two rows with those given in the last two illustrates that neither solvated electrons and solvated metal cations nor the $[M(en)_3^+ \cdot e^-@(en)_n]$ ion pairs are computed as being the most stable species.

The third row shows that formation of free metal anions, M^-, along with solvated metal cations, $M(en)_3^+$, is endothermic in the gas phase. Macroscopic solvation stabilizes the charged species. However, for the larger metals the magnitude of ΔE_{solv} is quite small. Perhaps formation of the solvated cation and the solvated anion is preferred? The fourth row illustrates that with the exception of the lightest alkali, this reaction is even less likely to occur in solution than the third. A comparison of the energies of numerous reactions suggests that niether the formation of solvated electrons nor of genuine metal anions is the most exothermic reaction. In fact, the fifth entry shows that in the gas phase two neutral noninteracting $M(en)_3$ complexes have a lower energy than any of the other species considered so far. However, the last two rows illustrate that the most exothermic

Table 3. Gas-Phase Change in Energy, ΔE_{gas}, in kcal/mol, for the Reactions of 2M + 6(en) Yielding the Products Listed below[a]

	products	Li	Na	K	Rb	Cs
1	$M(en)_3^+ + e^-@(en)_3 + M$	14.5 (−12.5)	29.4 (−1.2)	32.4 (4.4)	38.1 (9.5)	39.4 (10.9)
2	$[M(en)_3^+ \cdot e^-@(en)_3] + M$	−47.1 (−18.8)	−27.4 (0.9)	−26.2 (−5.1)	−16.9 (5.0)	−15.4 (6.5)
3	$M^- + M(en)_3^+ + 3(en)$	6.4 (−13.0)	21.0 (−16.1)	24.8 (−7.5)	31.3 (−3.2)	32.8 (−0.1)
4	$M(en)_3^+ + M(en)_3^-$	−33.5 (−21.6)	−1.8 (1.0)	3.5 (5.5)	17.2 (17.5)	20.6 (20.7)
5	$2[M(en)_3]$	−86.7 (−28.3)	−53.1 (−4.5)	−45.6 (0.9)	−31.7 (13.8)	−27.5 (17.3)
6	$[M(en)_3]_2$	**−95.5** (**-45.2**)	**−61.7** (−20.3)	**−54.0** (−15.1)	**−40.5** (2.5)	**−36.5** (2.3)
7	$[M(en)_3^{\delta+} \cdot M^{\delta-}] + 3(en)$	−61.9 (−37.4)	−44.3 (**-27.6**)	−36.3 (**-19.1**)	−28.6 (**-12.4**)	−26.3 (**-10.1**)

[a] The solution-phase values, ΔE_{solv}, are given in parentheses. The most exothermic reactions for a particular metal are highlighted in bold. Here, en = ethylenediamine and M = Li, Na, K, Rb, Cs.

dx.doi.org/10.1021/ja1085244 |J. Am. Chem. Soc. 2011, 133, 4829–4839

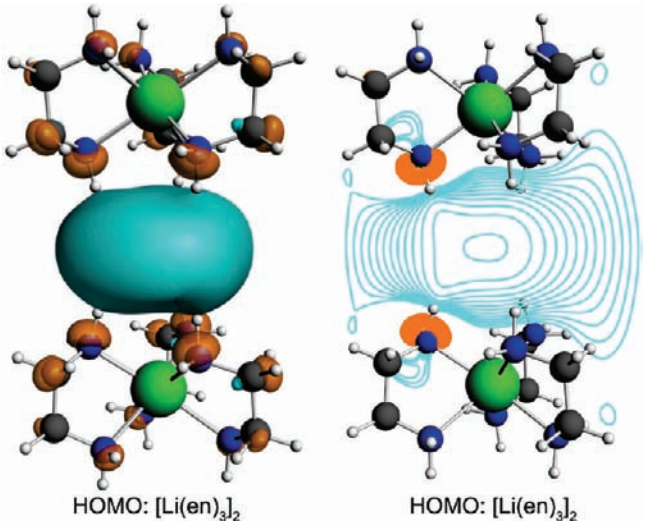

Figure 5. Isoprobability surface encompassing 30% of $|\Psi|^2$ of the $[Li(en)_3]_2$ HOMO with C_s symmetry ($|\Psi|^2$ = 90% is given in the Supporting Information). Also shown is the corresponding contour diagram where the plane of the contour passes through the lithium and one hydrogen atom on each superatom.

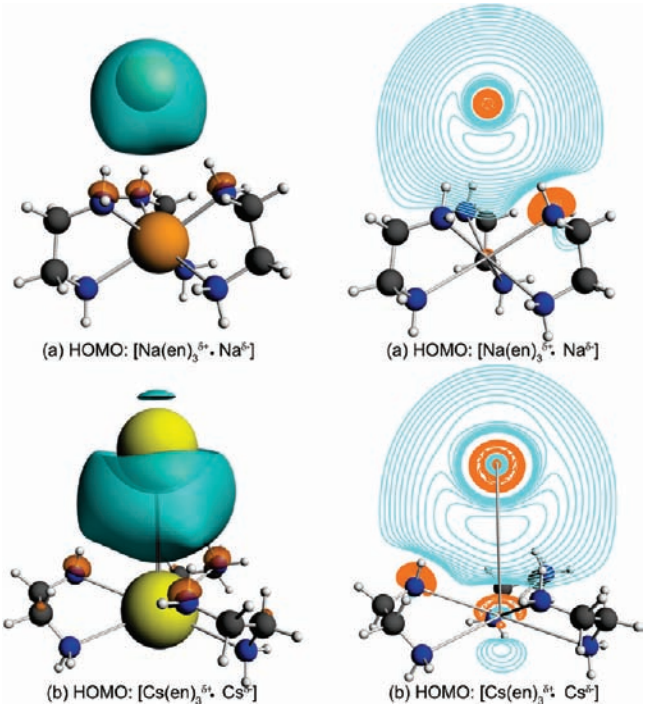

Figure 6. Isoprobability surfaces encompassing 30% of $|\Psi|^2$ of the HOMOs of (a) $[Na(en)_3^{\delta+}\cdot Na^{\delta-}]$ and (b) $[Cs(en)_3^{\delta+}\cdot Cs^{\delta-}]$ with C_3 symmetry ($|\Psi|^2$ = 90% is given in the Supporting Information). Also shown are the corresponding contour diagrams where the plane of the contour passes through the two metal atoms and a single nitrogen. In the contour diagrams, the metal atoms have been omitted for clarity. The HOMOs of $[M(en)_3^{\delta+}\cdot M^{\delta-}]$ with M = K, Rb are not shown since they were qualitatively similar.

reactions in both the gas and the solution phase yield the $[M(en)_3]_2$ dimer or an intriguing entity which we denote by the formula $[M(en)_3^{\delta+}\cdot M^{\delta-}]$. These may be integral constituents of alkali metal−ethylenediamine solutions and will be looked at in detail below.

3.3. $[M(en)_3]_2$: A Superalkali Dimer. The original definition of a superatom (it has recently been extended) pertained to clusters whose electronic structure and/or properties resembled those of the elements.[72] Classic examples of superatoms include the superhalogens Al_{13}[73,74] and Al_{14}[74] as well as the $Al_4H_7^-$[75] and $AlPb_{10}^+/AlPb_{12}^+$[76] clusters. It has even been shown that the Al_{13} superhalogen and the K_3O and Na_3O superalkalis can be used to make superatom assemblies.[77] What type of "clusters of clusters" could be constructed from the $M(en)_3$ superalkalis studied in this work?

Our previous DFT computations showed that it was energetically favorable for $[Li(NH_3)_4]_2$ dimers with paired spins ($S = 0$) to form from the interaction of two $Li(NH_3)_4$ monomer units.[5] The bond strength was calculated as being ~8 kcal/mol, and it was proposed that one may even think of $[Li(NH_3)_4]_2$ as "pseudo-H_2". The sixth row of Table 3 shows that in the gas phase the $[M(en)_3]_2$ dimers were found to be the most stable species out of any that were considered. The starting geometries were chosen so as to maximize the bonding interactions between the monomeric units, and a singlet electronic configuration was assumed. The magnitude of ΔE_{solv} was substantially lower than that of ΔE_{gas}. When solvation was taken into account another complex was more favorable for all of the metals other than lithium.

For the lightest alkali $[Li(en)_3]_2$ was the most stable species in the gas and solution phases. An isoprobability surface and contour diagram of its doubly occupied HOMO is illustrated in Figure 5. Clearly, it is made up from an overlap of the $Li(en)_3$ SOMOs (Figure 3b). The contour diagram shows that the maximum electron density is between the two superatoms, suggesting that this dimer can also be thought of as expanded Li_2. However, the monomer is not as spherical as $Li(NH_3)_4$, and the strength of the bond is likely to depend upon the relative orientation of the two monomer units. In the gas phase the bond strength for this particular orientation of $[Li(en)_3]_2$ and (all of the previously considered isomers of) $[Li(NH_3)_4]_2$ is roughly the same, about one-half the value we calculate for Li_2 (19.3 kcal/mol). The gas-phase dimerization energy for the $[M(en)_3]_2$ systems was found to be relatively metal independent.

3.4. $[M(en)_3^{\delta+}\cdot M^{\delta-}]$: A Mixed Superalkali−Alkali Dimer. In addition to homonuclear alkali metal dimers, mixed ones such as NaK and LiNa are also known. Accordingly, the geometries of dimers consisting of a single $M(en)_3$ superatom along with one alkali metal atom were optimized. Examination of the seventh row of Table 3 reveals that for all of the alkalis other than lithium the mixed dimers, denoted as $[M(en)_3^{\delta+}\cdot M^{\delta-}]$, were found to be the most stable in solution. The HOMOs of two of these (M = Na,Cs) illustrated in Figure 6 are representative of those obtained for the other metals. From visual inspection alone it appears that the valence MOs are composed of the SOMOs of $M(en)_3$ and the alkali metal valence s orbitals. Indeed, the interaction diagram for the $[Na(en)_3^{\delta+}\cdot Na^{\delta-}]$ mixed dimer in Figure 7 confirms this suspicion. The computed interaction diagrams for the heavier metals (not shown) also support this conclusion.

These results suggest that a covalent bond forms between the $M(en)_3$ superalkali and the alkali metal atom. Indeed, there is a build up of charge between the two. Yet, the charge density is not evenly distributed, so that a small amount, δ, is transferred from the superatom to the atom. From a Hirschfield charge analysis, this amount is estimated to be about 0.3 in the gas phase for all of the metals studied. Solvation effects stabilize charged species, so

dx.doi.org/10.1021/ja1085244 |J. Am. Chem. Soc. 2011, 133, 4829–4839

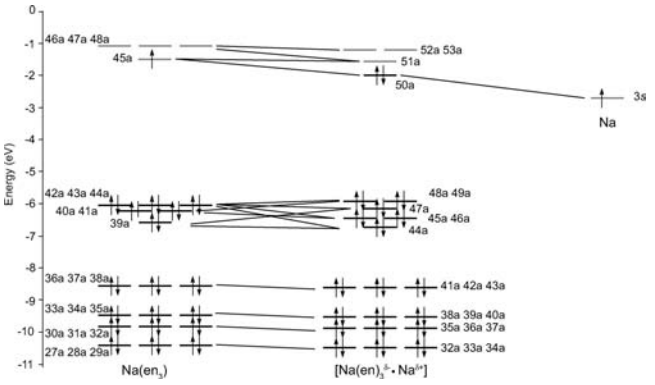

Figure 7. Interaction diagram for the formation of $[Na(en)_3^{\delta+} \cdot Na^{\delta-}]$ from $Na(en)_3$ and Na. The HOMO of $[Na(en)_3^{\delta+} \cdot Na^{\delta-}]$ is illustrated in Figure 6a. The analogous diagrams for the $[M(en)_3^{\delta+} \cdot M^{\delta-}]$ mixed dimers with M = K, Rb, Cs are not shown since they gave qualitatively similar results.

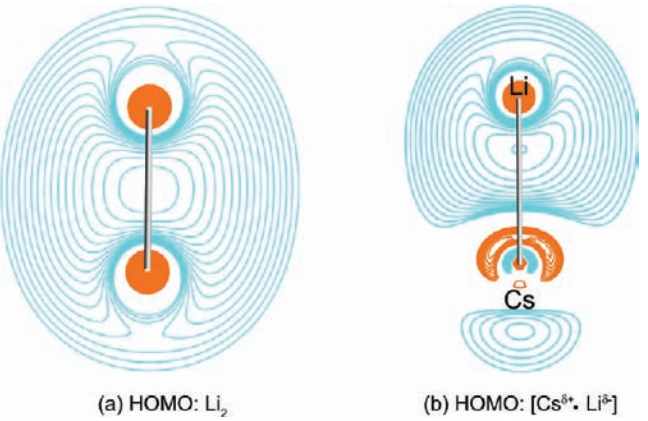

Figure 8. Contour diagrams of the HOMOs of the (a) Li_2 dimer and (b) CsLi mixed alkali dimer.

that in solution $\delta \approx 0.5$, and the distance between the atom and superatom also increases slightly. This is the reason for the $[M(en)_3^{\delta+} \cdot M^{\delta-}]$ notation used herein. The bond between the alkalis and the superalkalis is somewhat stronger than for the superalkali dimers considered above. It varies between 12.5 and 18.5 kcal/mol and 18.7 and 25.3 kcal/mol in the gas and solution phases, respectively, and in general is greater in magnitude for the smaller alkalis.

We also considered the energies for the disproportionation reactions

$$[M(en)_3^{\delta+} \cdot M^{\delta-}] \rightarrow M + M(en)_3 \quad (1)$$

$$[M(en)_3^{\delta+} \cdot M^{\delta-}] \rightarrow M^- + M(en)_3^+ \quad (2)$$

in the gas phase and in solution. In the gas phase reaction 2 is substantially more endothermic than reaction 1 (59−77 kcal/mol as compared with 19−29 kcal/mol). Since solvation stabilizes charged species, in the solution phase the opposite is found. A number of single-point computations where the distance between the anionic and cationic centers in $[Na(en)_3^{\delta+} \cdot Na^{\delta-}]$ is increased have been performed. As the two centers are pulled further apart the energy rises, $\delta \rightarrow 0$ in the gas phase and $\delta \rightarrow 1$ in the solution phase.

Electrical conductivities of Na, Rb, K, and Cs in ethylenediamine have been used to study the association between the ions present in solution,[78] and the conductance of sodium and cesium solutions in methylamine have been measured.[79] Could it be that there is a dynamic equilibrium between the species on the left and those on the right-hand side of reaction 2? That is, could one think of the $[M(en)_3^{\delta+} \cdot M^{\delta-}]$ complex as an ion pair composed of an alkali metal anion and a solvated cation? The solution-phase energies for reaction 2 are computed as being endothermic by 24.4 (Li), 11.5 (Na), 11.6 (K), 9.3 (Rb), and 10.0 kcal/mol (Cs). Due to various parameters in the COSMO calculations we estimate that there is an error of a few kcal/mol in these reaction energies. Moreover, it is the free energy change which will determine the direction and magnitude of the equilibrium. At first glance it may appear that entropic effects will favor the right-hand side, due to an increase in the degrees of freedom. On the other hand, the ionic species will induce the solvent around them to become more ordered, thereby decreasing the total entropy of the solution. Thus, it is difficult to predict by how much the entropy will affect the free energy and how the latter will change as a function of the temperature, pressure, and concentration of the solution. Molecular dynamics calculations will be useful in shedding light on the nature of this equilibrium.

3.5. Alkalis and Superalkalis. Whereas the lighter alkalis can be stored in oil, the heavier ones must be sealed in glass tubes so as to prevent violent reaction with air. To put it another way, as the radius of the alkali metal increases, its ionization energy decreases from 5.4 to 3.9 eV (Li−Cs). As expected, the values of the ionization energies calculated herein (using Koopman's theorem) are too low but follow the same trends going from 3.2 eV for Li to 2.2 eV for Cs. Since the $M(en)_3$ superalkalis have been expanded so that they have a larger radial extent than the alkalis themselves, one would expect them to be even more reactive. The computed ionization energies of $M(en)_3$ vary from 1.6 to 1.4 eV in going from M = Li to Cs. Figure 4 shows that the "radius" of the smallest superalkali $Li(en)_3$ is about 1.5 Å greater than that of Cs.

Out of all of the alkali metals the computed gas-phase dimerization energy is found to be biggest for sodium (21.4 kcal/mol) and smallest for cesium (13.0 kcal/mol). For the $[M(en)_3]_2$ superalkali dimers, this value is rather constant, on average about 8.7 kcal/mol. In general, it appears that the larger the monomer, the lower the energy of dimerization. A contour diagram depicting the HOMO of the $[Li(en)_3]_2$ superalkali dimer in Figure 5 bears a striking visual resemblance to the HOMO of Li_2 illustrated in Figure 8a. In going from the dimer to the superdimer, the distance between the two metal centers is expanded from 2.73 to 8.03 Å. For comparison, the metal−metal distance in Cs_2 falls in between these two values at 4.84 Å.

Also fascinating is the case of the mixed alkali dimers. A contour diagram of one of these, CsLi in Figure 8b, illustrates that the maximum in the charge density along the Li−Cs bond lies closer to the smaller, more electropositive lithium atom. The formula for the dimer may be written as $[Cs^{\delta+} \cdot Li^{\delta-}]$, where δ is estimated as being about 0.2 from the computed Hirschfield charges. Calculations on the other mixed-metal dimers indicate that the larger the difference between the radii of the two alkalis, the greater the δ. The strength of the bond of the mixed alkali dimers varies from 10.9 kcal/mol (CsRb) to 17.6 kcal/mol (NaLi) in the gas phase.

These findings are completely in line with the results presented for the $[M(en)_3^{\delta+} \cdot M^{\delta-}]$ mixed superalkali−alkali

dx.doi.org/10.1021/ja1085244 |J. Am. Chem. Soc. 2011, 133, 4829–4839

dimers. The HOMOs illustrated in Figure 6 show that the maximum charge density along the bond will be closer to the smaller, less electronegative atom. Moreover, since the size difference between the superalkalis and the alkalis is greater than between the alkalis themselves, the charge transferred, $\delta \approx 0.3$, is somewhat bigger than the one calculated for $[Cs^{\delta+}\cdot Li^{\delta-}]$. The bond strength of 12.6−18.5 kcal/mol for M = Cs−Li is comparable to the one computed for the mixed alkali dimers.

3.6. Optical Absorption Spectra. One of the most intriguing aspects of alkali−ethylenediamine solutions is their metal-dependent optical absorption spectra shown in Figure 9a.[13] In fact, for all of the metals other than lithium, the presence of alkali metal anions was put forward to account for the metal-dependent bands.[28−31] Because the intense band in the lithium solutions at 8000 cm^{-1} is similar to the absorption spectrum obtained for virtually all dilute MAS, it was proposed that mixtures of lithium in ethylenediamine give rise only to solvated electrons and Li^- does not form. The shoulders in the spectra obtained for the K, Rb, and Cs solutions were attributed to solvated electrons as well, whereas the main band was thought to result from the alkali metal anions. The spectrum of the Na solution exhibited only a single intense band ascribed to Na^-, and as a consequence it was suggested that solvated electrons do not form when sodium is mixed with ethylenediamine. At the time the assignments were made it was not possible to verify them by carrying out realistic first-principles computations.

We wondered how well the computed spectra of the most stable species proposed herein, $[Li(en)_3]_2$ and $[M(en)_3^{\delta+}\cdot M^{\delta-}]$ (M = Na, K, Rb, Cs), compare with those obtained experimentally. Our previous work indicated that the COSMO surface may affect the long-range tails of the diffuse orbitals, thereby artificially influencing the spectra, so gas-phase computations were considered. Recently, it has been shown that TD-DFT calculations employing a long-range corrected functional can qualitatively reproduce the spectrum of the aquated electron.[14] Here, we used a range-separated hybrid functional, CAM-B3LYP, in order to compute the vertical excitation energies. The simulated spectra in Figure 9b agree well with those obtained experimentally. The computed maxima in the absorption 15 200, 12 350, 11 800, and 11 700 cm^{-1} are in very good agreement with the experimental values of 15 400, 11 900, 11 600, and 10 500 cm^{-1} which were previously attributed to Na^-, K^-, Rb^-, and Cs^-,[9] suggesting that these peaks may be explained by the presence of $[M(en)_3^{\delta+}\cdot M^{\delta-}]$ (M = Na, K, Rb, Cs) instead. The shoulders in the simulated spectra of the K, Rb, and Cs superalkali−alkali mixed dimers are in reasonable agreement with experiment as well. The most notable difference between the calculated and experimental spectra is the fact that the energy at which the maximum absorption in the superdimer $[Li(en)_3]_2$ occurs is about 3000 cm^{-1} (0.37 eV) too low. Another discrepancy is that the calculated spectrum for $[Na(en)_3^{\delta+}\cdot Na^{\delta-}]$ has a shoulder, whereas the corrected experimental one does not. Nonetheless, the agreement between the two sets of spectra is good, especially taking into account that there might be other chromophores which we have not considered.

The spectra of the $[M(en)_3^{\delta+}\cdot M^{\delta-}]$ species are composed of numerous excitations with substantial oscillator strengths and are shown in the Supporting Information. The spectrum of $[Li(en)_3]_2$ is simpler to understand. One intense transition is from the s-like HOMO into a p-like orbital whose nodes coincide with the mirror plane passing between the two superalkalis. There are two

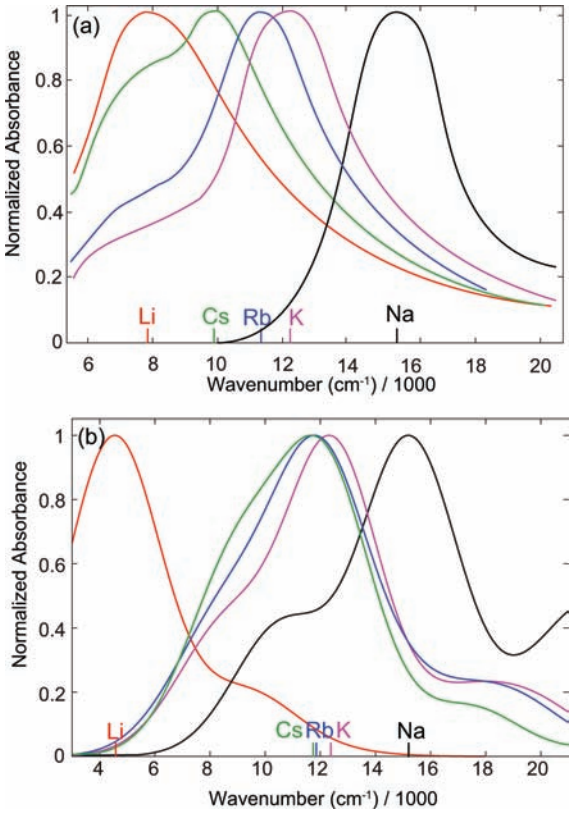

Figure 9. (a) Experimental optical spectra of alkali metals in ethylenediamine. Data taken from ref 13. The spectra have been corrected for the presence of a band at 650 nm, attributed to Na^+ obtained by exchange of the alkali cations with the sodium borosilicate glass used to prepare the solutions.[80] (b) Gas-phase absorption spectra of $[Li(en)_3]_2$, $[Na(en)_3^{\delta+}\cdot Na^{\delta-}]$, $[K(en)_3^{\delta+}\cdot K^{\delta-}]$, $[Rb(en)_3^{\delta+}\cdot Rb^{\delta-}]$, and $[Cs(en)_3^{\delta+}\cdot Cs^{\delta-}]$ simulated using a Gaussian broadening of 0.2 eV. Note that the scale on the two plots differs slightly. The maximum absorption is denoted by a colored tick mark on the *x* axis.

more intense, nearly degenerate transitions in which the excitation is to a p-like orbital whose node bisects both Li atoms. The calculated energy differences between the ob_3 and lel_3 conformers are minimal, suggesting that all four $M(en)_3$ isomers will be present in solution. The spectra in Figure 9 have been obtained for the $[M(en)_3^{\delta+}\cdot M^{\delta-}]$ and $[Li(en)_3]_2$ complexes containing the lel_3 conformer. The analogous computations for the ob_3 species have also been carried out verifying that the excitation energies, oscillator strengths, and simulated spectra are relatively independent of the orientation of the chelate rings. This is in line with previous results, which showed that the electronic CD spectrum of $[Co(en)_3]^{3+}$ is not particularly sensitive to the conformation of the ligands.[67]

3.7. Nuclear Magnetic Resonance Parameters. Another experimental tool which has been used extensively to interrogate alkalis in various solvents is NMR.[33−37,39,81] In fact, it was NMR data which first led to the conclusion that the sodide is a genuine metal anion and that the interaction of the anion with its environment increases going down group I. These experiments showed that the shielding of Na^- in various solvents differs by no more than 2 ppm from that of the gaseous Na atom.[39] On the other hand, this difference was slightly larger for K^- (−6.9 ppm), even bigger for Rb^- (−14.4 to −26.6 ppm, depending upon the solvent), and substantially greater for Cs^- (−52.3 ppm).

Table 4. Difference between the Shielding Constants (ppm) of the (a) Negatively and Positively Charged Metals in the $[M(en)_3^{\delta+}\cdot M^{\delta-}]$ Superalkali−Alkali (SA) Complex, (b) Genuine Alkali anion (A) and Complexed Cation (CC), (c) Negatively Charged Alkali in the SA Complex and the Genuine anion, (d) Positively Charged Metal in the SA Complex and in the Complexed Cation[a]

M	$\delta(-_{SA}/+_{SA})^b$	$\delta(-_A/+_{CC})^c$	$\delta(-_{SA}/-_A)^d$	$\delta(+_{SA}/+_{CC})^e$
Li	13.1	14.3	−1.0	0.1
Na	68.3	69.9	−5.9	−4.3
K	138.1	129.9	−17.4	−25.7
Rb	251.6	257.6	−40.9	−34.8
Cs	394.6	408.0	−97.0	−83.6

[a] The metal atoms for which the difference in shieldings is calculated are highlighted in bold in the footnotes to this table. [b] $\delta(-_{SA}/+_{SA}) = \sigma([M(en)_3^{\delta+}\cdot M^{\delta-}]) - \sigma([\mathbf{M}(en)_3^{\delta+}\cdot M^{\delta-}])$. [c] $\delta(-_A/+_{CC}) = \sigma(\mathbf{M}^-) - \sigma(\mathbf{M}(en)_3^+)$. [d] $\delta(-_{SA}/-_A) = \sigma([M(en)_3^{\delta+}\cdot \mathbf{M}^{\delta-}]) - \sigma(\mathbf{M}^-)$. [e] $\delta(+_{SA}/+_{CC}) = \sigma([\mathbf{M}(en)_3^{\delta+}\cdot M^{\delta-}]) - \sigma(\mathbf{M}(en)_3^+)$.

The shieldings of M^-, M^+, and of the metal centers in the $[M(en)_3^{\delta+}\cdot M^{\delta-}]$ and $M(en)_3^+$ species have been computed. This discussion focuses on the results obtained for the *lel*$_3$ conformers. The shieldings of the alkali metals in the *ob*$_3$ complexes differed by less than 1%, indicating that the NMR signals observed will not be influenced much by the orientation of the chelate rings. Only gas-phase results were considered, since the shieldings for both the free and the complexed alkalis were found to depend strongly on the radii used in the COSMO calculations, highlighting again the problem of constructing a suitable solvent cavity for systems with diffuse electron densities. In order to avoid calculations of NMR parameters for systems with unpaired electrons (which are not very accurate), we consider the nuclear magnetic shielding difference between M^- and M^+ instead of between M^- and the neutral gaseous metal atom. The computed estimates of $\sigma(M^-)_g - \sigma(M^+)_g$ for the gaseous alkali metal ions alone (9.1, 7.9, 5.9, 6.2, and 5.7 ppm going down group I) compare well with those derived from the data given in ref 39 (9.2, 8.1, 6.5, 6.0, and 5.4 ppm). The good agreement between these two sets of values suggests that the computational methods employed should provide relatively robust shielding differences for the other compounds considered.

The first column in Table 4 lists the difference between the anionic and the cationic resonances of the metal centers in the superalkali−alkali mixed dimers, $[M(en)_3^{\delta+}\cdot M^{\delta-}]$. Interestingly, these values are very similar to the difference between the shielding of a free metal anion, M^-, and the cationic metal center in $M(en)_3^+$ (second column). This suggests that these NMR signals alone cannot be used to determine if the third or the seventh reaction in Table 3 is more likely to occur. Moreover, the difference between the cationic and the anionic signals is insufficient to distinguish between species on the right (anions and solvated cations) or on the left (the $[M(en)_3^{\delta+}\cdot M^{\delta-}]$ ion pairs) side of reaction 2 in section 3.4.

The third column indicates that the difference between the shielding of M^- and the negatively charged alkali metal in $[M(en)_3^{\delta+}\cdot M^{\delta-}]$ is nearly negligible for Li. For Na it is a little bit larger, −5.9 ppm, and it increases steadily going down the group so that for Cs the difference is −97 ppm. At first glance these results seem to indicate that the interaction of the anionic and cationic metal centers in the mixed dimers increases with increasing radius of the metal atom, in complete agreement with the findings of ref 39. A similar conclusion can be reached from examining the fourth column which compares the resonances of the cationic metal center in the superalkali−alkali dimer with that in the $M(en)_3^+$ cationic complex. However, ΔE_{solv} for the reaction $M(en)_3 + M \rightarrow [M(en)_3^{\delta+}\cdot M^{\delta-}]$ is −23.2, −25.3, −19.5, −19.3, and −18.7 kcal/mol in going from Li to Cs, suggesting that the strength of the alkali−superalkali bond is about the same for all of the systems considered. Even though the sodium anion in $[M(en)_3^{\delta+}\cdot M^{\delta-}]$ is bound, its NMR chemical shielding is very similar to that of a genuine metal anion. In addition, even though the strength of the bond in the $[Cs(en)_3^{\delta+}\cdot Cs^{\delta-}]$ complex is about the same as that for the sodide, the NMR parameters are quite different from those of a gaseous Cs^-. At the present moment, it is not clear to us why the shieldings of the lighter alkalis seem to depend little on their environment whereas the heavier alkalis/superalkalis are strongly perturbed by bonding with $M(en)_3$/M. In a further study we will use orbital-based analysis techniques similar to those presented in ref 82 in order to get a better understanding of the origin of these shieldings.

In order to obtain a first-order estimate of the shielding difference between the anionic metal center in $[M(en)_3^{\delta+}\cdot M^{\delta-}]$ and the gaseous metal atom, M, the values provided in the third column will be employed. The experimental results indicate that this difference is solvent dependent for the larger alkalis, and none of the data from ref 39 was obtained in ethylenediamine. Even if the shielding of M could be computed reliably, our findings could not be compared with those of Pyper and Edwards directly. Nonetheless, in both sets of data the trends are clear. For Na the difference in the shieldings is only a few ppm and increases going down the group, being an order of magnitude larger for Cs. Thus, the computed differences between the shieldings of gaseous alkali anions, M^-, and the anionic alkali metal centers in $[M(en)_3^{\delta+}\cdot M^{\delta-}]$ are in good agreement with the results obtained by Pyper and Edwards, providing further evidence that for all of the metals other than lithium alkali−superalkali complexes may be important constituents of alkali−ethylenediamine solutions.

4. CONCLUSIONS

Humphry Davy's experiments were the first to hint that studies of alkali metals dissolved in various solvents will yield colorful results. We considered the peculiar case of ethylenediamine whose optical absorption spectra have led to the suggestion that the alkali metals may have three oxidation states: the usual 0 and +1 along with the exotic oxidation state of −1.

Static gas- and solution-phase DFT calculations have been carried out on a variety of species which could potentially be present in alkali−ethylenediamine solutions. The computed energies for a number of possible reactions showed that solvated electrons and alkali metal anions are energetically not the most stable species in these mixtures. Instead, clusters based upon the chiral $M(en)_3$ (M = Li−Cs) coordination complexes of D_3 symmetry were found to be particularly important. The quasi-spherical SOMOs of these molecular building blocks were made up largely in part from the diffuse unoccupied ligand orbitals as well as from the occupied and unoccupied s orbitals on the alkali metal atoms. Parallels were drawn to the tetrahedral $Li(NH_3)_4$ system studied previously.[5] It was pointed out that these building blocks may be viewed as superatoms, and in particular superalkalis, or expanded alkalis. The radius of the smallest superalkali

$Li(en)_3$ was estimated as being ~1.5 Å larger than that of cesium and its ionization potential even lower.

The $[Li(en)_3]_2$ superalkali dimer and superalkali−alkali complexes with the formula $[M(en)_3^{\delta+}\cdot M^{\delta-}]$ (M = Na, K, Rb, Cs), were found to be the most stable species. The latter can also be thought of as an ion pair formed from an alkali metal anion (M^-) and a solvated cation ($M(en)_3^+$). Striking similarities were illustrated between $[Li(en)_3]_2$ and the alkali metal dimer Li_2 as well as $[M(en)_3^{\delta+}\cdot M^{\delta-}]$ and the mixed-metal dimer CsLi. Our computations revealed that clusters based upon superalkali building blocks are likely to be important constituents of alkali metal−ethylenediamine solutions.

The most intense peaks in the computed optical absorption spectra of $[M(en)_3^{\delta+}\cdot M^{\delta-}]$ (M = Na−Cs) agreed well with the signals that have been previously attributed to the alkali metal anions. The maximum absorption in the spectrum of $[Li(en)_3]_2$ occurred at an energy that was somewhat lower than the peak that has been previously ascribed to solvated electrons, yet the difference was not untypical of the error that can be expected from TD-DFT computations. Overall, the simulated optical absorption spectra of the most stable species are in good agreement with the experimental spectra, which has previously been interpreted as providing evidence for Na^-, K^-, Rb^-, Cs^-, and solvated electrons. NMR parameters were also computed for the mixed-metal superalkali−alkali dimers. The difference between the shielding of gaseous M^- and the anionic metal center in $[M(en)_3^{\delta+}\cdot M^{\delta-}]$ showed that for the heavier alkalis the environment perturbs the NMR resonances to a greater degree than it does for the lighter ones, in complete agreement with experiment.

Humphry Davy was the first to isolate sodium and potassium. Our computations suggest that the series he uncovered may be further expanded to the $M(en)_3$ superalkalis, building blocks of the complexes likely to be present in solutions made up of alkali metals and ethylenediamine.

■ ASSOCIATED CONTENT

Supporting Information. Geometries and formation energies of the $e^-@(en)_n$ clusters and the $[Li(en)_3^+\cdot e^-@(en)_n]$ (n = 1, 3, 6) ion pairs; isoprobability surfaces encompassing 90% of $|\Psi|^2$ for selected MOs; simulated gas- and solution-phase absorption spectra of the free alkali metal anions; simulated gas-phase absorption spectra of the $[Li(en)_3]_2$ and $[M(en)_3^{\delta+}\cdot M^{\delta-}]$ (M = Na, K, Rb, Cs) complexes; Cartesian coordinates and energies of the species studied in this work; complete author list for refs 40 and 56. This material is available free of charge via the Internet at http://pubs.acs.org.

■ AUTHOR INFORMATION

Corresponding Author
ezurek@buffalo.edu

■ ACKNOWLEDGMENT

The author acknowledges support from the Center of Computational Research at SUNY Buffalo, and the useful comments and suggestions of the referees.

■ REFERENCES

(1) Edwards, P. P. *Adv. Inorg. Chem. Radiochem.* **1982**, *25*, 135–185.
(2) Holton, D.; Edwards, P. *Chem. Br.* **1985**, *21*, 1007–1013.
(3) Thomas, J. M.; Edwards, P. P.; Kuznetsov, V. L. *ChemPhysChem* **2008**, *9*, 59–66.
(4) Weyl, W. *Ann. Phys.* **1864**, *121*, 606–612.
(5) Zurek, E.; Edwards, P. P.; Hoffmann, R. *Angew. Chem., Int. Ed.* **2009**, *48*, 8198–8232.
(6) Shkrob, I. A. *J. Phys. Chem. A* **2006**, *110*, 3967–3976.
(7) Chandra, A.; Marx, D. *Angew. Chem., Int. Ed.* **2007**, *46*, 3676–3679.
(8) Dye, J. L. *Sci. Am.* **1977**, *237* (1), 92−105.
(9) Dye, J. L.; DeBacker, M. G. *Annu. Rev. Phys. Chem.* **1987**, *38*, 271–301.
(10) Wagner, M. J.; Dye, J. L. *Annu. Rev. Mater. Sci.* **1993**, *23*, 223–253.
(11) Dye, J. L. *Inorg. Chem.* **1997**, *36*, 3816–3826.
(12) Dye, J. L. *Science* **2003**, *301*, 607–608.
(13) Dye, J. L. *Acc. Chem. Res.* **2009**, *42*, 1564–1572.
(14) Jacobson, L. D.; Herbert, J. M. *J. Am. Chem. Soc.* **2010**, *132*, 10000–100002.
(15) Williams, C. F.; Herbert, J. M. *J. Phys. Chem. A* **2008**, *112*, 6171–6178.
(16) Larsen, R. E.; Glover, W. J.; Schwartz, B. J. *Science* **2010**, *329*, 65–69.
(17) Marsalek, O.; Uhlig, F.; Frigato, T.; Schmidt, B.; Jungwirth, P. *Phys. Rev. Lett.* **2010**, *105*, 043002.
(18) Blades, H.; Hodgins, J. W. *Can. J. Chem.* **1955**, *33*, 411–425.
(19) Douthit, R. C.; Dye, J. L. *J. Am. Chem. Soc.* **1960**, *82*, 4472–4478.
(20) Burow, D. F.; Lagowski, J. J. *Adv. Chem. Ser.* **1965**, *50*, 125.
(21) Thompson, J. C. *Electrons in Liquid Ammonia*; Oxford University Press: Oxford, 1976.
(22) Lindner, J.; Unterreiner, A. N.; Vöhringer, P. *ChemPhysChem* **2006**, *7*, 363–369.
(23) Dye, J. L.; DeBacker, M. G.; Dorfman, L. M. *J. Chem. Phys.* **1970**, *52*, 6251–6258.
(24) Harris, R. L.; Lagowski, J. J. *J. Phys. Chem.* **1980**, *84*, 1091–1096.
(25) Jortner, J. *J. Chem. Phys.* **1959**, *30*, 839–846.
(26) Copeland, D. A.; Kestner, N. R.; Jortner, J. *J. Chem. Phys.* **1970**, *53*, 1189–1216.
(27) Varriale, L.; Tonge, N. M.; Bhalla, N.; Ellis, A. M. *J. Chem. Phys.* **2010**, *132*, 161101.
(28) Hurley, I.; Tuttle, T. R. J.; Golden, S. In *Metal-Ammonia Solutions*; Lagowski, J. J., Sienko, M. J., Eds.; Colloque Weyl II, Ithaca, New York, 1969; Butterworths, London, 1970; pp 449−480.
(29) Matalon, S.; Golden, S.; Ottoleng, M. *J. Phys. Chem.* **1969**, *73*, 3098–3101.
(30) DeBacker, M. G.; Dye, J. L. *J. Phys. Chem.* **1971**, *75*, 3092–3096.
(31) Lok, M. T.; Dye, J. L.; Tehan, F. J. *J. Phys. Chem.* **1972**, *76*, 2975–2981.
(32) Dewald, R. R.; Dye, J. L. *J. Phys. Chem.* **1964**, *68*, 121–127.
(33) Ceraso, J. M.; Dye, J. L. *J. Chem. Phys.* **1974**, *61*, 1585–1587.
(34) Dye, J. L.; Andrews, C. W.; Ceraso, J. M. *J. Phys. Chem.* **1975**, *79*, 3076–3079.
(35) Edwards, P. P.; Ellaboudy, A.; Holton, D. M. *Nature* **1985**, *317*, 242–244.
(36) Holton, D. M.; Edwards, P. P.; Johnson, D. C.; Page, C. J.; McFarlane, W.; Wood, B. *J. Am. Chem. Soc.* **1985**, *107*, 6499–6504.
(37) Ellaboudy, A.; Holton, D. M.; Pyper, N. C.; Edwards, P. P.; Wood, B.; McFarlane, W. *Nature* **1986**, *321*, 684–685.
(38) Concepcion, R.; Dye, J. L. *J. Am. Chem. Soc.* **1987**, *109*, 7203–7204.
(39) Pyper, N. C.; Edwards, P. P. *J. Am. Chem. Soc.* **1986**, *108*, 78–81.
(40) Baerends, E. J. et al. *ADF2010.01*; SCM, Theoretical Chemistry, Vrije Universiteit: Amsterdam, The Netherlands, URL http://www.scm.com.
(41) te Velde, G.; Bickelhaupt, F. M.; Baerends, E. J.; Fonseca Guerra, C.; van Gisbergen, S. J. A.; Snijders, J. G.; Ziegler, T. *J. Comput. Chem.* **2001**, *22*, 931–967.
(42) Perdew, J. P.; Burke, K.; Wang, Y. *Phys. Rev. B* **1996**, *54*, 16533–16539.

(43) Zhang, Y.; Yang, W. *Phys. Rev. Lett.* **1998**, *80*, 890.
(44) Perdew, J. P.; Burke, K.; Ernzerhof, M. *Phys. Rev. Lett.* **1998**, *80*, 891.
(45) Hammer, B.; Hansen, L. B.; Norskov, J. K. *Phys. Rev. B* **1999**, *59*, 7413–7421.
(46) Vosko, S. H.; Wilk, L.; Nusair, M. *Can. J. Phys.* **1980**, *58*, 1200–1211.
(47) van Lenthe, E.; Baerends, E. J.; Snijders, J. G. *J. Chem. Phys.* **1993**, *99*, 4597–4610.
(48) van Lenthe, E.; Baerends, E. J.; Snijders, J. G. *J. Chem. Phys.* **1994**, *101*, 9783–9792.
(49) van Lenthe, E. Ph.D. thesis, Vrije Universiteit Amsterdam: Amsterdam, The Netherlands, 1996.
(50) Cohen, A. J.; Mori-Sanchés, P.; Yang, W. *Science* **2008**, *321*, 792–794.
(51) Mierzwicki, K.; Latajka, Z. *Chem. Phys.* **2001**, *265*, 301–311.
(52) van Gisbergen, S. J. A.; Snijders, J. G.; Baerends, E. J. *Comput. Phys. Commun.* **1999**, *118*, 119–138.
(53) van Gisbergen, S. J. A.; Kootstra, F.; Schipper, P. R. T.; Gritsenko, O. V.; Snijders, J. G.; Baerends, E. J. *Phys. Rev. A* **1998**, *57*, 2556–2571.
(54) Yanai, T.; Tew, D. P.; Handy, N. C. *Chem. Phys. Lett.* **2004**, *393*, 51–57.
(55) Govind, N.; Valiev, M.; Jensen, L.; Kowalski, K. *J. Phys. Chem. A* **2009**, *113*, 6041–6043.
(56) Bylaska, E. J. et al. *NWChem, A Computational Chemistry Package for Parallel Computers*, Version 5.1.1 (2008); Pacific Northwest National Laboratory: Richland, WA, 2008.
(57) Weigend, F.; Ahlrichs, R. *Phys. Chem. Chem. Phys.* **2005**, *7*, 3297–3305.
(58) Klamt, A.; Schüürmann, G. *J. Chem. Soc., Perkin Trans. 2* **1993**, 799–805.
(59) Klamt, A. *J. Phys. Chem.* **1995**, *99*, 2224–2235.
(60) Klamt, A. *J. Phys. Chem.* **1996**, *100*, 3349–3353.
(61) Pye, C. C.; Ziegler, T. *Theor. Chem. Acc.* **1999**, *101*, 396–408.
(62) Haranczyk, M.; Gutowski, M. *J. Chem. Theory. Comput.* **2008**, *4*, 689–693.
(63) Schreckenbach, G.; Ziegler, T. *J. Phys. Chem.* **1995**, *99*, 606–611.
(64) Schreckenbach, G.; Ziegler, T. *Theor. Chem. Acc.* **1998**, *99*, 71–82.
(65) Dyall, K.; van Lenthe, E. *J. Chem. Phys.* **1999**, *111*, 1366–1372.
(66) Autschbach, J.; Zheng, S. *Annu. Rep. NMR Spectrosc.* **2009**, *67*, 1–95.
(67) Autschbach, J.; Jorge, F. E.; Ziegler, T. *Inorg. Chem.* **2003**, *42*, 2867–2877.
(68) Freedman, T. B.; Cao, X.; Young, D. A.; Nafie, L. A. *J. Phys. Chem. A* **2002**, *106*, 3560–3565.
(69) Irikura, K. K. *J. Phys. Chem. A* **2008**, *112*, 983–988.
(70) Rencsok, R.; Kaplan, T. A.; Harrison, J. F. *J. Chem. Phys.* **1993**, *98*, 9758–9764.
(71) Stacy, A. M.; Edwards, P. P.; Sienko, M. J. *J. Solid State Chem.* **1982**, *45*, 63–70.
(72) Castleman, A. W.; Khanna, S. N. *J. Phys. Chem. C* **2009**, *113*, 2664–2675.
(73) Bergeron, D. E.; Castleman, A. W.; Morisato, T.; Khanna, S. N. *Science* **2004**, *304*, 84–87.
(74) Bergeron, D. E.; Roach, P. J.; Castleman, A. W.; Jones, N. O.; Khanna, S. N. *Science* **2005**, *307*, 231–235.
(75) Roach, P. J.; Reber, A. C.; Woodward, W. H.; Khanna, S. N.; Castleman, A. W. *Proc. Natl. Acad. Sci* **2007**, *104*, 14565–14569.
(76) Neukermans, S.; Janssens, E.; Chen, Z. F.; Silverans, R. E.; Schleyer, P. v. R.; Lievens, P. *Phys. Rev. Lett.* **2004**, *92*, 163401(1−4).
(77) Reber, A. C.; Khanna, S. N.; Castleman, A. W. *J. Am. Chem. Soc.* **2007**, *129*, 10189–10194.
(78) Dewald, R. R.; Dye, J. L. *J. Phys. Chem.* **1964**, *68*, 128–134.
(79) Dewald, R. R.; Browall, K. W. *J. Phys. Chem.* **1970**, *74*, 129–133.
(80) Hurley, I.; Tuttle, T. R. J.; Golden, S. *J. Chem. Phys.* **1968**, *48*, 2818–2819.
(81) Edwards, P. P. *J. Phys. Chem.* **1984**, *88*, 3772–3780.
(82) Autschbach, J. *J. Chem. Phys.* **2008**, *128*, 164112–11.